



20th IAEA Fusion Energy Conference
Vilamoura, Portugal, 1 to 6 November 2004

IAEA-CN-116/EX/P3-14

**EDGE STABILITY AND PERFORMANCE OF THE
ELM-FREE QUIESCENT H-MODE AND THE
QUIESCENT DOUBLE BARRIER MODE ON DIII-D**

W.P. WEST, K.H. BURRELL, T.A. CASPER,¹ E.J. DOYLE,² P.B. SNYDER,
P. GOHIL, L.L. LAO, C.J. LASNIER,¹ A.W. LEONARD, M.F.F NAVE,³
T.H. OSBORNE, D.M. THOMAS, G. WANG,² and L. ZENG²

General Atomics
San Diego, California 92186-5608
United States of America

¹Lawrence Livermore National Laboratory, Livermore, California, USA

²University of California, Los Angeles, California, USA

³Associação Euratom/IST, Instituto Superior Técnico, Lisbon, Portugal

This is a preprint of a paper intended for presentation at a scientific meeting. Because of the provisional nature of its content and since changes of substance or detail may have to be made before publication, the preprint is made available on the understanding that it will not be cited in the literature or in any way be reproduced in its present form. The views expressed and the statements made remain the responsibility of the named author(s); the views do not necessarily reflect those of the government of the designating Member State(s) or of the designating organization(s). In particular, neither the IAEA nor any other organization or body sponsoring this meeting can be held responsible for any material reproduced in this preprint.

Edge Stability and Performance of the ELM-Free Quiescent H-Mode and the Quiescent Double Barrier Mode on DIII-D

W.P. West,¹ K.H. Burrell,¹ T.A. Casper,² E.J. Doyle,³ P.B. Snyder,¹ P. Gohil,¹
L.L. Lao,¹ C.J. Lasnier,² A.W. Leonard,¹ M.F.F Nave,⁴ T.H. Osborne,¹
D.M. Thomas,¹ G. Wang,³ and L. Zeng³

¹General Atomics, P.O. Box 85608, San Diego, California 92186-5608, USA

²Lawrence Livermore National Laboratory, Livermore, California, USA

³University of California, Los Angeles, California, USA

⁴Associaçao Euratom/IST, Instituto Superior Tecnico, Lisbon, Portugal

e-mail contact of main author: west@fusion.gat.com

Abstract. The quiescent H (QH) mode, an edge localized mode (ELM)-free, high-confinement mode, combines well with an internal transport barrier to form quiescent double barrier (QDB) stationary state, high performance plasmas. The QH-mode edge pedestal pressure is similar to that seen in ELMing phases of the same discharge, with similar global energy confinement. The pedestal density in early ELMing phases of strongly pumped counter injection discharges drops and a transition to QH-mode occurs, leading to lower calculated edge bootstrap current. Plasmas current ramp experiment and ELITE code modeling of edge stability suggest that QH-modes lie near an edge current stability boundary. At high triangularity, QH-mode discharges operate at higher pedestal density and pressure, and have achieved ITER level values of β_{PED} and v^* . The QDB achieves performance of $\beta_{\text{NH}89} \sim 7$ in quasi-stationary conditions for a duration of $10 \tau_E$, limited by hardware. Recently we demonstrated stationary state QDB discharges with little change in kinetic and q profiles ($q_0 > 1$) for 2 s, comparable to ELMing “hybrid scenarios”, yet without the debilitating effects of ELMs. Plasma profile control tools, including electron cyclotron heating and current drive and neutral beam heating, have been demonstrated to control simultaneously the q profile development, the density peaking, impurity accumulation and plasma beta.

1. Introduction

The achievement of a high-performance ELM-free H-mode [1,2,3] has important implications for burning plasma devices such as ITER. ELMs represent a serious operational limit for ITER. In today’s tokamaks, long-pulse stationary-state plasmas are produced which meet or exceed the plasma performance, in normalized parameters, needed for ITER to meet its goals. In most cases, these high performance plasmas are accompanied by repetitive edge collapses, called ELMs, which produce large particle and heat pulses that propagate rapidly to the divertor strike plates. Empirical scaling studies of ELMs [4], supported by edge magnetohydrodynamic (MHD) theory [5], indicate that on ITER these heat pulses could be of sufficient intensity to ablate or melt any plasma facing material. The QH-mode is a demonstration that high performance plasmas with pedestal pressures equal to those in standard high confinement mode plasmas, yet with no ELMs, can be produced in stable, stationary-state conditions. When combined with an internal transport barrier to form a quiescent double barrier (QDB) discharges, performance levels comparable to the ELMing “hybrid” scenarios are achieved [6].

In this paper we will report on: 1) properties of the QH pedestal and the progress made on QH-mode edge profile stability analysis, leading to an indication that ELM suppression results from a reduction of the edge bootstrap current compared to ELMing phases, 2) the observation of a deep and narrow radial electric field well at the edge of the plasma during QH-mode and 3) the advances in performance of the QDB discharges, including demonstrations of plasma profile control.

2. The QH-Mode Pedestal and Edge Stability

Research on the QH pedestal on DIII-D has focused on determining the reason for ELM stabilization. The QH edge was previously shown to have a pressure and pressure gradient very similar to ELMing H-mode but it has different density and temperature gradients

compared to ELMing H-mode, and these lead to a significantly lower calculated edge bootstrap current in QH. This lower edge current is a strong candidate for the stabilization of ELMs, a hypothesis supported by edge current perturbation experiments. Preliminary modeling of the edge stability to coupled peeling/ballooning modes using the measured electron and ion density and temperature profiles in high resolution equilibrium reconstructions including the edge bootstrap current indicates that QH-mode is near marginal stability. Edge stability experiments and modeling will be discussed in more detail in the remainder of Section 2.

2.1. QH-Mode Pedestal Profiles

Plasma profiles from the vicinity of the pedestal are shown in Fig. 1 from a strongly pumped upper single-null QH discharge with average triangularity, ~ 0.46 . Edge electron density and temperature profiles are measured with very good spatial resolution in the region of the separatrix and H-mode pedestal using the DIII-D Thomson scattering system [7]. The profiles of C^{+6} temperature, toroidal and poloidal rotation, and density are measured with good spatial resolution using the DIII-D charge exchange recombination (CER) system [8]. Because QH-mode is a quiescent and stationary operating state, data can be taken from an extended period of time for a precise profile fit. Figure 1 (a,b) shows fits to data from a 200 ms window centered at 3000 ms in shot 106919 [9]. The electron density and temperature are fit to a modified tanh function [10] while the ion temperature data are fit to a cubic spline. The mapping of the spatial location of the Thomson and CER channels to the magnetic flux function ψ is done using the equilibrium reconstruction code, EFIT [11]. The fits from the QH phase are compared to fits from the ELMing phase of this discharge at 1210 ms, approximately half way between two ELMs. The pressure profiles for the ELMing and QH phases are very similar, but the density is lower in the QH phase and the temperatures are higher. The density behavior reflects the general trend that QH-mode is initiated from an ELMing phase as the density drops due to strong pumping.

In discharges with an H-mode-like pedestal, the edge current is comprised primarily of the neoclassical bootstrap current [12,13], J_{BOOT} , driven by the sharp edge gradients in density and temperature.

$$J_{BOOT} = \alpha \frac{\partial n_e}{\partial \rho} + \beta \frac{\partial T_e}{\partial \rho} + \gamma \frac{\partial T_i}{\partial \rho} \quad . \quad (1)$$

The gradients are taken with respect to the toroidal flux coordinate, ρ , and the coefficients α , β , and γ are functions of the plasma shape and collisionality. Typically, $\alpha > \beta > \gamma$, i.e., the density gradient is the strongest driver for the edge current. Edge gradients are shown in Fig. 1, along with the calculated edge bootstrap current for the ELMing and QH phases of this discharge [9]. While the pressure gradients are essentially identical, the edge bootstrap current, driven mostly by the density gradient, is much larger in the ELMing phase. Since high and medium n coupled peeling/ballooning modes with a dominant peeling like character are known to be driven unstable by increasing edge current, this result led to the hypothesis

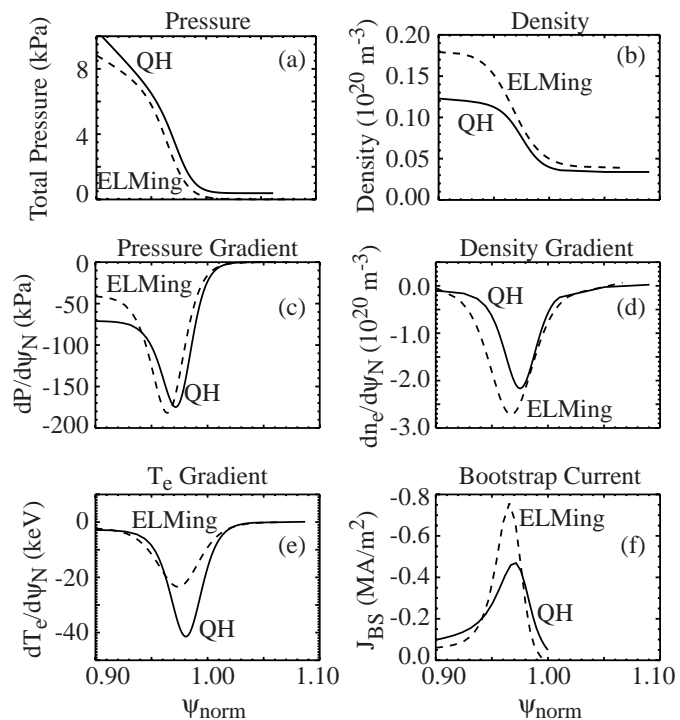


FIG. 1. Edge density and pressure profiles and their gradients and the resulting J_{BOOT} during QH and ELMing phases of the same discharge.

that the ELMs in the early phase of this discharge are a current driven instability, and the reduction in edge bootstrap current due to the reduced edge density gradient is responsible for the stabilization of ELMs.

2.2. Edge Stability Modeling

The nonlinear growth of coupled peeling/ballooning modes [6] is the leading candidate for the underlying MHD mechanism governing ELMs. ELITE-code [6] modeling has been initiated to evaluate the linear growth rate of these modes in QH-mode discharges. Equilibria with high resolution pressure and current profiles near the separatrix are produced using the CORSICA code [14], which includes the NCLASS model [15] to calculate the edge bootstrap current. A high triangularity, $\delta=0.8$, high elongation, $\kappa=2$, double null QH discharge with relatively high edge pedestal density ($2.9 \times 10^{19} \text{ m}^{-3}$) and pressure ($1.8 \times 10^4 \text{ kPa}$) has been studied. These highly shape QH discharges routinely result in higher pedestal density and pressures compared to upper single null QH-modes with lower average triangularity of 0.46 [1,16]. The edge current profile and pressure gradient from the CORSICA equilibrium is shown in Fig. 2a). ELITE modeling indicates the equilibrium to be marginally stable to peeling/ballooning modes. To evaluate the proximity of the equilibrium to a stability limit, several equilibria with small perturbations of the pressure and current profiles away from the initial equilibrium were constructed using CORSICA. A stability diagram derived from ELITE modeling of these equilibria is shown in Fig. 2b). The ‘x’ in the diagram is the location of the experimental case, and is stable. Solid blue squares represent perturbed cases that are shown to be stable, while solid yellow, orange, and red cases are unstable with progressively larger predicted linear growth rates. CORSICA equilibria produced with a j_{edge} above that of the experimental case exhibit a magnetic shear reversal in the edge which complicates the stability analysis. Current ramp experiments discussed in the next section suggest that QH-modes operate just below the j_{edge} stability limit, as indicated by the upper location of the line. The stability limit in this discharge extends to high j_{edge} and p' due to the strong shaping.

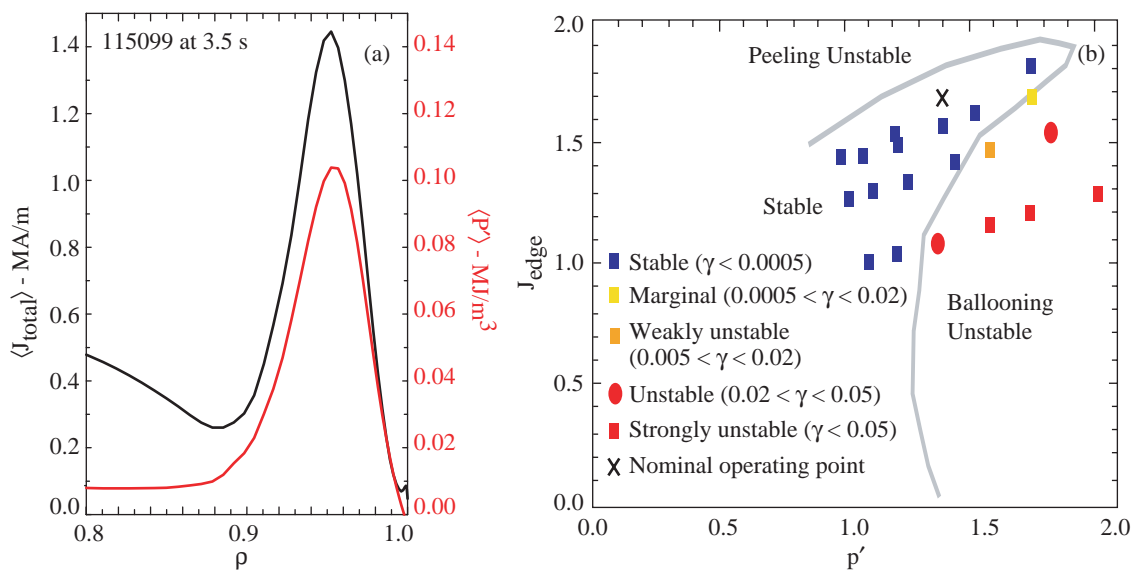


FIG. 2. The edge current density and pressure gradient, (a), from the CORSICA equilibrium for a high shaped QH-mode discharge used as the basis for the stability diagram shown in (b). The grey line in (b) shows that stability boundary. The upper limit at high j_{edge} is suggested by the current ramp experiments discussed in Section 2.3.

2.3. The EHO and ELMs During Current Ramps

Inductive ramps of the plasma current, carried out during QH-mode operation as a method to test the stability of QH-mode to perturbation of the edge current, indicate that QH-mode lies near an edge current stability boundary. Since the edge of QH-mode plasmas are low

density and hot, the resistivity is low and inductive I_p ramps transiently alter the edge current density without having a significant effect on the interior current. Inductive ramps, both increasing and decreasing I_p magnitude, have been carried out in discharges after establishing QH-mode operation. Ramp rates were varied from 0.1 to 0.5 MA/s. A return to an ELMing state was observed during ramps of increasing I_p magnitude, but ELMs did not appear during the downward ramps.

Time traces of the plasma current, chord integrated density, \dot{B} probe and divertor D_α monitor for a downward I_p ramp at 0.5 MA/s are shown in Fig. 3. ELMs are apparent in the D_α monitor prior to 1400 ms, but disappear when the QH-mode starts. QH is accompanied by continuous MHD activity, usually a coherent mode with multiple harmonics known as the edge harmonic oscillation (EHO), apparent in the \dot{B} signal prior to the current ramp. Within 40 ms after the start of the downward I_p ramp, the EHO changes nature and decreases significantly in amplitude. After 200 ms the EHO activity reappears but disappears after another 200 ms. During the time that the EHO is absent, the chord integrated plasma density is increasing, shown in Fig. 3. A close examination of the plasma density and temperature profiles indicate that in the vicinity of the pedestal ($\psi_{\text{norm}} \sim 0.95$) there is little change in the plasma density, temperature and pressure or their gradients. However inside the pedestal, starting at $\psi_{\text{norm}} \leq 0.91$, the plasma pressure increases significantly. The total kinetic pressure near $\psi_{\text{norm}} \sim 0.91$ is shown as a function of time in Fig. 3. In the absence of the EHO, the plasma pressure rises until D_α activity increases slightly and the EHO reappears.

Data from an upward I_p ramp at 0.15 MA/s is shown in Fig. 4. Again the EHO is apparent prior to the ramp, and remains vigorous for about 50 ms, but then is suddenly terminated by an ELM. The EHO returns in just several ms, but is again terminated by an ELM. The \dot{B} signal at higher time resolution is shown in the vicinity of an ELM in Fig. 4. The EHO is constant in size and frequency until the sudden growth of magnetic disturbance during $\sim 250 \mu\text{s}$ resulting in the ELM. Similar behavior is seen in discharges with 0.2 and 0.5 MA/s upward ramps. Chord integrated density is not changing during the early EHO-ELM-EHO cycles, but detailed profiles are not well resolved on this time scale by available Thomson and CER data.

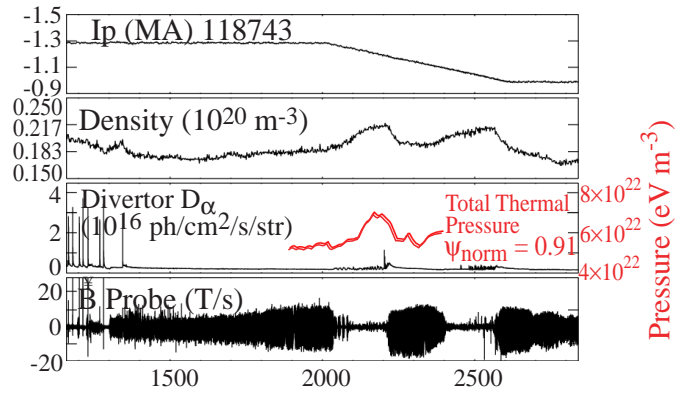


FIG. 3. Time traces of a magnetic B probe, divertor D_α monitor, chord averaged density, and edge pressure at $\psi=0.91$ during a ramp down of I_p .

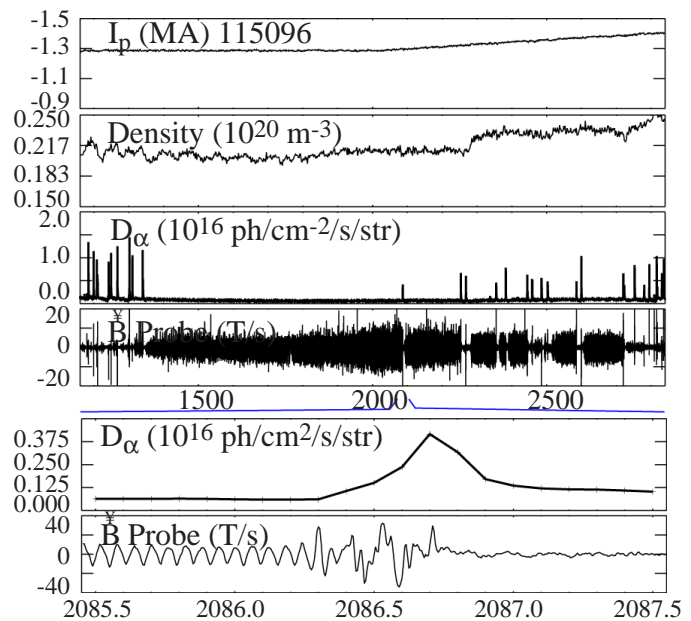


FIG. 4. Time traces of a magnetic B probe, divertor D_α monitor, chord averaged density, during a ramp up of I_p . The B probe, divertor D_α monitor are shown at higher time resolution in the bottom two panels.

These experiments support the conclusion from Sec. 2.1 that the QH-mode is residing very near a current driven stability limit, leading to the placement of the stability boundary at high j_{edge} shown in Fig. 2.

2.4. Pedestal Ion Collisionality and β

The motivation to understand how ELMs are stabilized, and to develop ELM-free high performance scenarios comes from the ITER design effort, since standard high performance scenarios exhibit ELMs, which may be very destructive to the first wall. It is especially interesting that QH-mode has simultaneously achieved pedestal collisionality [17] and β values equal to those expected in the ITER $q=5$ scenario, as shown in Table 1. These values of pedestal ion collisionality and β were achieved in the high triangularity double-null shapes with relatively high pedestal density as discussed in Section 2.2.

Table 1

Shot	ν_i^*	β_{ped}	$H_{\text{ITER-89P}}$	Z_{eff}	ν_e^*
115056	0.085	1.96	1.61	1.99	0.23
118820	0.077	1.55	1.82	2.11	0.20
ITER	0.084	1.59	1.8	1.65	0.11

3. Radial Electric Field Well During QH-mode

A narrow and deep radial electric field, E_r , well is observed at the edge of QH-mode discharges [1]. Although the theory of the role of edge rotation on edge stability is not well developed, this strong E_r well may play some role in the edge stability. In addition, evidence of prompt fast ion loss to the outer wall has been reported [18,19], and modeled for these counter injected discharges. Recent experiments have demonstrated that prompt loss is not a key element of QH-mode or of the E_r well. Prompt loss due to the outwardly directed banana orbits of beam ions birthed in the edge of the plasma is expected for four of the seven neutral beam injectors on DIII-D, which we denote as tangential, or T-beams. Ions from the other three neutral beam injectors, which inject at more somewhat more perpendicular direction (P-beams), are not promptly lost [20]. QH-mode discharges with long duration of only P-beam injection were recently demonstrated [9]. QH-mode was initiated and sustained for significant (>1 s) duration during P-beam only injection.

The edge radial electric field well was measured during QH-discharges with T-beam only and P-beam only injection [16]. We take advantage of the fact that QH-mode can be stationary for long durations to enhance the already excellent spatial resolution of the CER system by slowing scanning the edge of the plasma across the CER viewing chords. The radial electric field well during both T and P beam injection is shown in Fig. 5. These measurements demonstrate that the prompt fast ion loss calculated for T-beam injection does not play a dominant role in either the radial electric field, or in the formation of QH-mode. However it was observed that QH-mode formed more readily and lasted longer in T-beam dominated discharges.

4. The High-Performance Quiescent Double Barrier

In addition to studies of the QH-mode edge, QDB operation has been investigated, with emphasis on plasma profile and impurity control [1–3,21,22]. Near-steady QDB plasma conditions have been maintained on DIII-D for up to 4 s, as indicated in Fig. 6, corresponding to greater than $35\tau_E$. In general, QDB discharges exhibit relatively high stored energies with $\beta_N \leq 3$ and neutron production rates $S_n \leq 5.5 \times 10^{16} \text{ s}^{-1}$. DIII-D QDB plasmas have been included in a recent international study of high-performance hybrid and AT regimes from AUG, DIII-D, JET, JT-60U and TS [6], where the results demonstrate that QDB performance is highly competitive in terms of fusion gain $[(H_{89} \times \beta_N) / q_{95}^2]$ and normalized duration (τ_D / τ_E) . Near-steady, high performance QDB discharges allow us to address issues of critical

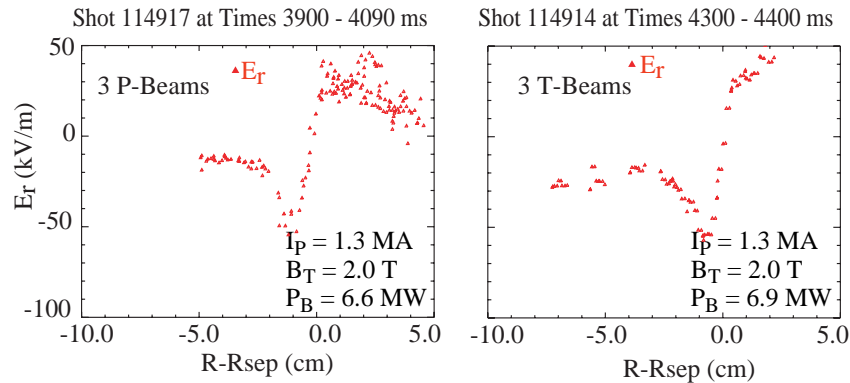


FIG. 5. The radial electric field, E_r , in T and P dominated discharges.

importance to maintenance and optimization of ITB discharges, such as current profile modification to maintain $q > 1$, and pressure profile modification for impurity profile control, using control tools such as electron cyclotron heating (ECH) and current drive (ECCD). Injection of EC power inside the ITB region successfully raised q_0 and q_{\min} , and also reduced the density peaking from $n_e/\langle n_e \rangle = 2$ to 1.5, accompanied by a significant reduction in the core carbon and high-Z impurities [3,22]. However, there was also a drop in total plasma stored energy with ECH application; while T_e increases, there is a reduction in T_i a slowing of the toroidal rotation (V_i), resulting in an overall drop in stored energy. Transport analysis indicates that both the electron and ion thermal diffusivities increase with the injection of EC power [23,24].

In more recent experiments the q -profile control has been demonstrated using ECCD. As shown in Fig. 6, the application of 2 MW of co-ECCD can arrest the secular decline of q_0 , such that that q_0 remains constant and above 1.5 for ~ 2 s during the EC pulse (q_{\min} behaves similarly but is not shown). Maintaining an elevated q_0 and q_{\min} is beneficial for increasing both the bootstrap fraction and plasma stability. As also shown in Fig. 6, with the application of higher neutral beam power q_0 is raised above 1.5, primarily due to the added neutral beam counter current drive that is peaked near the axis [3]. The current profile modification observed with EC/ECCD application is in agreement with modeling. The EC deposition radius and CD characteristics were systematically scanned inside the ITB, so as to explore the effects on the pressure and current profiles. The change in transport was found to depend weakly on the radial location of the resonance. Localized electron heating allows control of the electron temperature profile while also changing the density inside the barrier. The current drive modification is dependent on both the ECCD direction, e.g., co-, counter- or radial (no current drive) and on the radial deposition location. By separately aiming different EC antennas, current drive versus electron heating can be optimized. The magnitude of the change in transport, as evidenced by the change in density, is dependent on the injected power providing some control over profile modification. Similarly, by broadening the EC-deposition profile, control can be obtained of the magnetic shear and electron temperature profiles and stabilization of MHD has been observed [3].

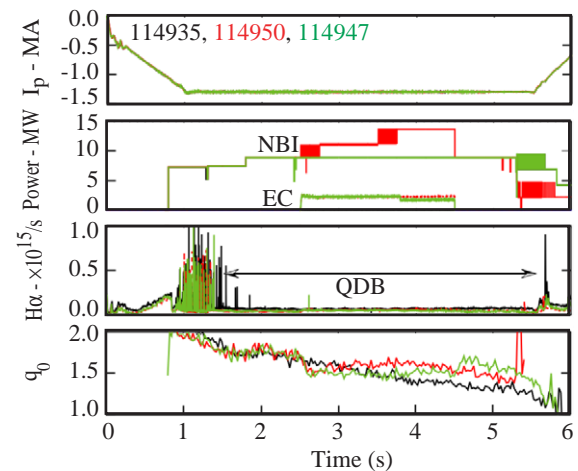


FIG. 6. Comparison of the evolution of q_0 for a QDB discharge with (114947) and without (114935) ECCD (2 MW). Also shown is 114950 with 2 MW ECCD and increasing NBI during the EC pulse.

The degradation of plasma density and stored energy due to the application of EC can be overcome using increased neutral beam injection (NBI). As shown in Fig. 7, increased neutral beam heating during the EC injection phase can recover EC-induced losses in several plasma parameters. With the application of an additional 2.5 MW of neutral-beam heating, plasma conditions (β_N , V_i , and T_i) return to near pre-EC values. An additional ~ 5 MW of neutral-beam power pushes T_e , T_i , β_N and the neutron rate above their pre-EC values, while the line-average density returns to its initial value of $2.2 \times 10^{19} \text{ m}^{-3}$ without a significant rise in core impurities. Finally, we note that these QDB discharges are quite robust to large changes in the injected power with no loss in the QH-mode character even with a 50% increase in the neutral beam heating and up to an addition of 3 MW of EC power, i.e. the plasma remains in a steady QDB state without returning to ELMing H-mode conditions.

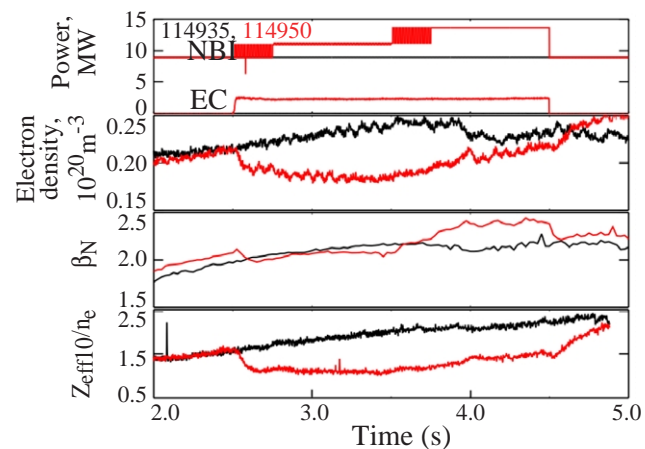


FIG. 7. Comparison of plasma performance parameters for discharges with constant and increasing NBI during the application of ECH for control of density, impurity, and current profiles.

5. Discussion and Conclusions

The QH-mode is a robust high-confinement mode of tokamak operation that exhibits no impulsive wall heat loading due to ELMs. This mode has been observed and investigated on most major tokamaks, including DIII-D, ASDEX-Upgrade [25], JT-60U [26] and JET [25]. When combined with an internal transport barrier to form the QDB-mode, long-pulse, near stationary-state operation is achieved with performance levels comparable to the ELMing “hybrid” mode. The quiescent long pulse character of this mode is ideal for some tokamak physics experiments, including the demonstration of profile control, both density and current control, using ECH/ECCD along with NBI. Recently other tokamak physics experiments, not discussed here, have taken advantage of the quiescent nature of the edge plasma to explore important core plasma physics that may be masked by the perturbative effects of ELMs, e.g., a study of cascade effects in core Alfvén wave activity [27].

The stability properties of the QH edge are just beginning to be explored. Stability modeling using the ELITE code to calculate the growth rate of coupled peeling/ballooning modes indicates that QH-mode lies near a current limited stability boundary at high j_{edge} and p' . Edge current perturbation experiments, as well as comparisons between QH and ELMing phases of the same discharge, indicate that the QH-mode is very near a current driven stability boundary, and small increases (decreases) in the edge current will provoke an ELM (temporarily relax the EHO). To date, QH-mode has only been observed in discharges with at least some counter injection. There are also observations of significant prompt fast ion loss in some QH-mode discharges, however the demonstration of QH-mode in discharges where prompt fast ion loss is not expected indicate no strong connection to QH-mode. A very narrow, deep radial electric field well exists just inside the separatrix in QH-mode. These observations suggest that the edge rotation and electric fields may be contributors to ELM stabilization in QH-mode, however the theory of edge stability is only beginning to incorporate the effects of rotation. QH studies on JT-60U [26], which has the capability of wide variation in the net momentum and energy input from their beam injection system, have shown a relationship between ELM rate and edge rotation.

QH- and QDB-modes remain both technically and scientifically interesting. The stabilization of ELMs in a high performance regime is of direct interest to ITER. The fact that

QH-mode is achieved at ITER relevant values of pedestal collisionality and β is a strong motivator for future QH-mode studies.

Acknowledgment

This work was supported by the U.S. Department of Energy under DE-FC02-04ER54698, W-7405-ENG-48, and DE-FG03-01ER54615.

References

- [1] BURRELL, K.H., et al., Phys. Plasmas **8** (2001) 2153.
- [2] GREENFIELD, C.M., et al., Phys. Rev. Lett. **20** (2001) 4544.
- [3] CASPER, T.A., et al., "Current drive and pressure profile modification with electron cyclotron power in DIII-D quiescent double barrier experiments," Proc. of the 30th EPS Conf. on Controlled Fusion and Plasma Physics, St. Petersburg, Russia (2003).
- [4] LOARTE, A., et al., J. Nucl. Mater. **313-316** (2003) 962.
- [5] SNYDER, P.B., et al., Phys. Plasmas **9** (2002) 2037.
- [6] SIPS, A.C.C., et al., paper IT/P3-36, these proceedings(2004).
- [7] CARLSTROM, T.N., CAMPBELL, G.L., DeBOO, J.C., Rev. Sci. Instrum. **63** (1992) 4901.
- [8] BURRELL, K.H., et al., Rev. Sci. Instrum. **72** (2001) 1028.
- [9] WEST, W.P., et al., Plasma Phys. Control. Fusion **46** (2004) A179.
- [10] GROEBNER, R.J., and OSBORNE, T.H., Phys. Plasmas **5** (1998) 1800.
- [11] LAO, L.L., et al., Nucl. Fusion **30** (1990) 1035.
- [12] THOMAS, D.M., et al., Phys. Rev. Lett. **93** (2004) 065003-1.
- [13] WADE, M.R., MURAKAMI, M., and POLITZER, P.A., Phys. Rev. Lett. **92** (2004) 235005-1.
- [14] CASPER, T.A., et al., Plasma Phys. Control. Fusion **45** (2003) 1193.
- [15] HOULBERG, W.A., et al., Phys. Plasmas **4** (1997) 3230.
- [16] BURRELL, K.H., et al., Plasma Phys. Control. Fusion **46** (2004) A179.
- [17] SAUTER, O., et al., Phys. Plasmas **6** (1999) 2834.
- [18] LASNIER, C.J., et al., J. Nucl. Mater. **313-316** (2003) 904
- [19] WEST, W.P., LASNIER, C.J., WATKINS, J.G., et al., "Fast ion loss to the plasma facing wall during quiescent H-modes on DIII-D." presented at the 16th Int. Conf. on Plasma Surface Interactions, Portland, Maine (2004) and accepted for publication, J. Nucl. Mater.
- [20] WEST, W.P., et al., "Quiescent H-mode, an ELM-Free High-Confinement Mode on DIII-D With Potential for Stationary State Operation" Proc. of the 30th EPS Conf. on Controlled Fusion and Plasma Physics, St. Petersburg, Russia (2003).
- [21] DOYLE, E.J., et al., Plasma Phys. and Control. Fusion **43** (2001) A95.
- [22] DOYLE, E.J., et al., Proc. 19th IAEA Fusion Energy Conference, Lyon, France (2002) EX/C3-2.
- [23] CASPER, T.A., et al., Proc. 29th EPS Conference on Controlled Fusion and Plasma Physics, Montreux, Switzerland (2002).
- [24] GREENFIELD, C.M., et al., Plasma Phys. and Control. Fusion **44** (2002) A123.
- [25] SUTTROP, W., et al., Plasma Phys. Control. Fusion **46** (2004) A151.
- [26] SAKAMOTO, Y., et al., Plasma Phys. Control. Fusion **46** (2004) A299.
- [27] NAZIKIAN, R., ALPER, B., BERK, H.L., et al., paper EX/5-1, these proceedings.